

Learning Structure Aware Deep Spectral Embedding

Hira Yaseen, Arif Mahmood

This is a draft version of the paper accepted in *IEEE Transactions on Image Processing*, 2023

Abstract—Spectral Embedding (SE) has often been used to map data points from non-linear manifolds to linear subspaces for the purpose of classification and clustering. Despite significant advantages, the subspace structure of data in the original space is not preserved in the embedding space. To address this issue subspace clustering has been proposed by replacing the SE graph affinity with a self-expression matrix. It works well if the data lies in a union of linear subspaces however, the performance may degrade in real-world applications where data often spans non-linear manifolds. To address this problem we propose a novel structure-aware deep spectral embedding by combining a spectral embedding loss and a structure preservation loss. To this end, a deep neural network architecture is proposed that simultaneously encodes both types of information and aims to generate structure-aware spectral embedding. The subspace structure of the input data is encoded by using attention-based self-expression learning. The proposed algorithm is evaluated on six publicly available real-world datasets. The results demonstrate the excellent clustering performance of the proposed algorithm compared to the existing state-of-the-art methods. The proposed algorithm has also exhibited better generalization to unseen data points and it is scalable to larger datasets without requiring significant computational resources.

Index Terms—Unsupervised learning, Subspace clustering, Spectral clustering, Deep spectral embedding, Self-expression learning.

I. INTRODUCTION

HIGH-DIMENSIONAL data often spans low-dimensional manifolds instead of being uniformly distributed across the ambient space. Recovering these low-dimensional manifolds reduces the computational cost, memory requirements, and the effect of noise and thus improves the performance of learning, inference, and recognition tasks. Subspace clustering refers to the problem of separating data according to their underlying manifolds. Subspace clustering algorithms have a wide range of applications in computer vision such as image clustering [1, 8, 11, 54], motion segmentation [53, 70], co-segmentation of 3D bodies [18, 69], DNA sequencing [58, 64], omics data clustering [9, 57], and gene expression [66]. Structure of a data is often encoded by using a self-expression matrix which is based on the observation that a data point in a union of subspaces can be efficiently represented by a combination of other data points in the same manifold. Over the years, many variants of the subspace clustering have been proposed such as LSR [39], LRR [37], SSC [11], LS3C [46], Kernel SSC [47], BDR [40], SC-LALRG [75], and S³COMP-C [8]. In these methods, the self-expression matrix has been computed using conventional optimization techniques. Recently, some algorithms have also used deep neural

networks for the computation of self-expression matrices such as DSC [20], PSSC [41], NCSC [83], S²ConvSCN [81], MLRDSC [25], MLRDSC-DA [1], DASC [84], SENet [82], and ODSC [59]. In all of these algorithms computation of self-expression matrices have been improved by using various constraints and this matrix is then utilized to construct the affinity matrix for spectral clustering. This arrangement works well if the data spans a union of linear subspaces however, the performance may degrade if the underlying space is a nonlinear manifold. Local neighborhood relationships are also ignored which were originally used for the construction of a fully connected graph and thus the strength of spectral embedding is not fully utilized. In the current work, we propose to integrate the strength of spectral embedding along with subspace structure preservation using the self-expression matrix. For this purpose, we propose a deep neural network-based architecture that learns embedding by simultaneous minimization of spectral embedding-based loss as well as ensuring self-expression property in the latent space.

The objective function of spectral clustering is to find an embedding of the data points by eigendecomposition of the laplacian matrix encoding pairwise similarities. That data representation is then clustered to assign them to different categories. Despite many advantages, the subspace structure of data in the original space is not preserved in the embedding space. Structure preservation during data transformation aims to keep a set of embeddings in a common subspace that shares the same subspace in the ambient space. To address this, many subspace clustering algorithms have been proposed. The assumption of data spanning linear subspaces made by these existing subspace clustering methods often gets violated in many real-world applications. The data may be corrupted by errors or because of missing trajectories, occlusion, shadows, and specularities [11]. These algorithms compute the self-expression coefficient matrix either using ℓ_1 -norm, ℓ_2 -norm, nuclear norm, or a combination of these norms to preserve data structure. However, local neighborhood information may be lost in these methods because the graph structure and local node connectivity are not included, resulting in sub-optimal clustering performance [65].

In the current work, we explicitly encode both the local and the global input data structures. For encoding the local structure, the supervision of spectral embedding is used to train a deep network preserving local neighborhood graph affinities of data points. For global data structure preservation, the learned embedding is constrained to minimize self-expression loss. The proposed neural architecture is trained in a batch-by-batch fashion by computing both spectral supervision and self-expression in batches. Compared to full data supervision as used by many existing techniques, our proposed approach

H. Yaseen and A. Mahmood are with the Department of Computer Science, Information Technology University (ITU), 346-B, Ferozpur Road, Lahore, Pakistan. E-mails: PhDCS17002@itu.edu.pk, arif.mahmood@itu.edu.pk

saves computational time & memory resources.

The existing self-expressiveness sparse representations may limit connectivity between data points belonging to the same subspace, which may not form a single connected component [8]. To handle this issue ℓ_2 -norm based dense solution has been proposed however it requires the underlying subspaces to be independent [77]. In the current work, we propose a self-attention-based global structure encoding technique. For this purpose, we use two multi-layer fully connected networks including a query net and a key net. These networks are learned by minimizing elastic net-constrained self-expression loss. The learned structure encoding matrix is made sparse by using a nearest-neighbor-based approach removing less probable links in latent space representations.

Overall the proposed algorithm consists of an end-to-end deep neural architecture that learns structure-aware deep spectral embedding via simultaneous minimization of a Laplacian eigenvector-based loss and a self-attention-based structure encoding loss. As the network gets trained, it iteratively learns the local and global structures of the input data. The proposed algorithm is applied on six publicly available datasets including EYaleB [12], COIL-100 [44], MNIST [28], ORL [52], CIFAR-100 [27], and ImageNet-10 [7], and compared with 51 SOTA methods including deep learning-based methods as well as traditional spectral and subspace clustering techniques. The proposed algorithm has consistently shown improved performance over the compared methods. The following are the main contributions of the current work:

- We propose to learn non-linear spectral embedding by using the supervision of eigenvectors of the graph Laplacian matrix.
- The learned embedding is constrained to be structure-aware by using a self-expression-based loss. For this purpose, a self-attention-based structure encoding is exploited.
- To reduce the complexity both the graph Laplacian and the self-expression matrices are computed batch by batch.
- The proposed deep embedding network is capable of finding effective representations for unseen data points thus enabling better generalization than the existing methods.

The rest of the paper is organized as follows: Section II contains related work, Section III presents the proposed methodology, and experiments are given in Section IV. Conclusions and future directions follow in Section V.

II. RELATED WORK

Due to numerous applications of subspace clustering in computer vision and related fields, several researchers have aimed to improve it in various dimensions such as reducing time complexity [17, 31], memory complexity [34, 56], learning self-expressive coefficients matrix to preserve the linear structure of data [20], while some others have intended to generalize it to unseen data [22, 55], and some others have tried to make it scalable [2, 8, 22]. Chen *et al.* [8] proposed random dropout in a self-expressive model to deal with the over-segmentation issues in traditional SSC algorithms. They also used a consensus algorithm to produce a scalable solution

over a set of small-scale problems using orthogonal matching pursuit. You *et al.* [76] introduced scalability by dealing with class-imbalanced data using a greedy algorithm that selects an exemplar subset of data using sparse subspace clustering. With the resurgence of deep learning in subspace clustering, many deep network-based methods have also been proposed.

Ji *et al.* [20] proposed a convolutional auto-encoder for reconstruction and introduced an additional fully connected self-expressive layer between latent-space data points. Zhang *et al.* [81] further extended the concept of a self-expressive trainable layer by incorporating spectral clustering to compute pseudo labels which are then used to train a classification layer using the latent space representation. Zhang *et al.* [83] collaboratively used two affinity matrices, one from a trainable self-expressive layer, and another from a binary classifier applying softmax on latent representations, to further improve the self-expression layer. Kheirandishfard *et al.* [24] implicitly trained DNN to impose a low-rank constraint on latent space and the self-expressive layer is then used to compute the affinity matrix. Valanarasu *et al.* [59] used over-complete and under-complete auto-encoder networks to get latent representations to input into a trainable self-expressive layer. Lv *et al.* [41] used weighted reconstruction loss and a learnable self-expressive layer to compute spectral clustering pseudo labels to be compared with the predictions of a classification layer on top of latent representations. These methods have reported excellent results, however, learning self-expressive coefficients matrix using a full dataset requires high memory complexity. Also if new unseen data points are added, these methods require computing a full self-expressive matrix. Therefore such methods are neither scalable to larger datasets nor generalizable to unseen data points.

Peng *et al.* [48] computed a prior self-expressive matrix from input data and used it to train an auto-encoder for structure preservation in the latent space. This method preserves structure however, it requires high computational & memory complexity to compute self-expressive matrix and train network using a full training dataset. Shaham *et al.* [55] proposed a DNN to embed input data points into the eigenspace of its associated graph Laplacian matrix. Despite using deep learning, orthogonality in latent space is ensured via QR decomposition instead of using the learning-based framework. Also, input data structure preservation is not explicitly enforced in the latent space.

In contrast to the existing algorithms, we propose to train our network using local neighborhood information using a fully connected graph in addition to the global structure of the data captured by the self-expressive matrix and the reconstruction loss. We use batch-wise training of a fully connected network to produce a subspace-preserving self-expressive matrix at input space enabling scalability to larger datasets and generalization to unseen data points.

III. PROPOSED STRUCTURE PRESERVING DEEP SPECTRAL CLUSTERING

In order to implement the proposed solution, we directly train an end-to-end network in a batch-by-batch fashion that

learns structure-aware spectral representations of data points. Once this network is trained, new unseen data points can be input into the network, and the corresponding embedding is computed. Since the network is supervised by spectral clustering-based loss, its brief overview is given below.

A. Batch-Based Spectral Clustering

Traditionally spectral clustering has been performed on all data simultaneously however, we propose spectral clustering to be performed on mini-batches and to combine the results using our proposed deep neural network. Compared to the existing methods such an approach would significantly reduce the computational and memory complexity. For this purpose, we divide a given dataset into a large number of random batches, each having m data points. Let $X = \{x_i\}_{i=1}^m \in \mathcal{R}^{n \times m}$ be a batch data matrix such that $x_i \in \mathcal{R}^n$ be a data point spanning n dimensional non-linear manifold. The data batch is mapped to a batch graph G_b having adjacency matrix $A_b \in \mathcal{R}^{m \times m}$ computed as follows:

$$A_b(i, j) = \begin{cases} \exp\left(-\frac{d_{i,j}^2}{2\sigma^2}\right) & \text{if } i \neq j \\ 0 & \text{if } i = j \end{cases} \quad (1)$$

where $d_{i,j}$ is some distance measure between data points x_i and x_j within the same batch, and in our work we consider $d_{i,j} = \|x_i - x_j\|_2$. The graph G_b contains an edge between all nodes (m_i, m_j) representing the local neighborhood, and parameter σ controls the width of the neighbourhood [63]. Laplacian matrix for the graph G_b is computed as $L_b = D_b - A_b$, and $D_b \in \mathcal{R}^{m \times m}$ is a batch based degree matrix defined as:

$$D_b(i, j) = \begin{cases} \sum_{j=1}^m A_b(i, j) & \text{if } i = j \\ 0 & \text{Otherwise.} \end{cases} \quad (2)$$

The Laplacian matrix L_b is semi-positive definite with at least one zero eigenvalue for a fully connected graph. Eigenvalue decomposition of L_b is given by: $L_b = U_b \Lambda_b U_b^\top$, where $U_b = \{u_i\}_{i=1}^m$ is a matrix of eigenvectors of L_b , such that $u_i \in \mathcal{R}^m$ are arranged in the decreasing order of eigenvalues: $v_m \geq v_{m-1} \geq \dots \geq v_2 \geq v_1$, and Λ_b is a matrix having these eigenvalues on the diagonal. For dividing the graph into k partitions, only k eigenvectors corresponding to the minimum non-zero k eigenvalues are considered. **If in a particular batch, the actual number of clusters is less than k , even then k eigenvectors are selected. Since the number of clusters is not directly used in the loss function, a varying number of clusters across batches has no effect on the training process.**

Let $U_k = \{u_i\}_{i=1}^k \in \mathcal{R}^{m \times k}$ be the matrix of these eigenvectors. The columns of U_k^\top represent an embedding of original data in a k dimensional space such that the embedding space is linear and therefore any linear clustering algorithm, **such as K-means**, will be able to reveal the groups in the original data. Thus spectral clustering can be considered a projection of data from high-dimensional nonlinear manifolds to low-dimensional linear subspaces. Since we perform spectral clustering batch by batch, to combine all batches to get a unified solution we propose to train a deep neural network to simulate spectral embedding. Such a spectral clustering method would

be scalable to significantly larger datasets without incurring computational or memory costs.

B. Structure Aware Spectral Embedding

For larger datasets having millions of data points, the size of the graph and the corresponding Laplacian matrix grows by $O(p^2)$, where p are the total data points. Eigendecomposition on such large matrices incurs a high computational cost. Therefore, traditional spectral clustering lacks scalability to larger datasets [38]. Similarly, applications with online data arrival require computing an embedding in the low dimensional space without going through the complete process which is also not possible with most of the existing methods. Our proposed solution addresses both of these issues and also incorporates the structure information within the spectral embedding. Fig. 1 shows all the important steps in our proposed Structure Aware Deep Spectral Embedding (SADSE) algorithm.

A simple strategy to simulate spectral clustering with an auto-encoder is to use the spectral embedding as a direct supervisory signal and train the network to minimize the error:

$$\min_{\theta_e} \|U_k^\top - Z_b\|_F^2, \quad (3)$$

where $Z_b = \{z_i\}_{i=1}^m \in \mathcal{R}^{k \times m}$ is a k -dimensional latent network embedding such that $k \ll n$, and θ_e are the encoder network parameters. We empirically observe that instead of training only an encoder network, simultaneously training a pair of encoder and decoder networks provides better initialization and improves accuracy. The encoder and decoder pair referred to as Auto-Encoder is used to project high dimensional data $x_i \in \mathcal{R}^n$ to low dimensional latent space $z_i \in \mathcal{R}^k$ and then back to the original space. The encoder may be considered as a nonlinear projector from a higher dimensional to a low dimensional space. Auto-Encoders are often trained to minimize the reconstruction error over a training dataset X_b :

$$\mathcal{L}_R := \min_{\theta_e, \theta_d} \sum_{i=1}^m \|x_i - \hat{x}_i\|_2, \quad (4)$$

where \hat{x}_i is the back-projected output of the decoder and θ_d are the parameters of the decoder network. Reconstruction loss aims to preserve the locality of input data space. We propose to train the deep auto-encoder such that the latent space Z_b be in some sense close to the low dimensional spectral embedding.

In the current work, instead of (3), we minimize both ℓ_1 and ℓ_2 losses between the latent space and spectral embedding as given below:

$$\mathcal{L}_S := \min_{\theta_e, \theta_d} \sum_{i=1}^m (\|x_i - \hat{x}_i\|_2 + \lambda_1 \|z_i - U_k^\top(i)\|_1 + \lambda_2 \|z_i - U_k^\top(i)\|_2) \quad (5)$$

where $U_k^\top(i)$ shows a column of U_k^\top consisting of the corresponding coefficients from the set of selected k eigenvectors, and λ_1 , and λ_2 are hyperparameters assigning relative weights to different loss terms, $\|\cdot\|_1$ shows ℓ_1 , and $\|\cdot\|_2$ is ℓ_2 norm. The ℓ_1 loss ensures the error is sparse while the ℓ_2 loss minimizes the distance between the latent space representation z_i and

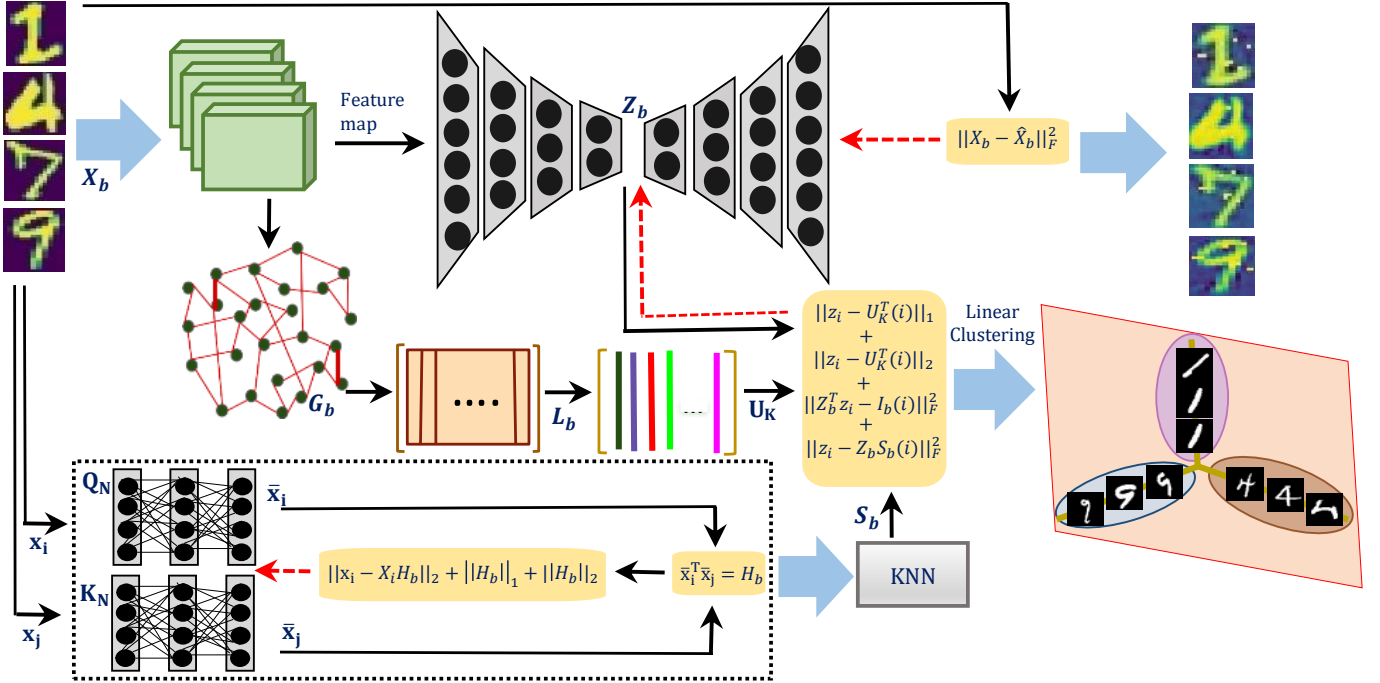


Fig. 1: The proposed Structure Aware Deep Spectral Embedding (SADSE) network is trained using self-expressiveness and spectral supervision. Batch data matrix X_b is input and the latent space matrix Z_b is constrained to minimize spectral loss and structural losses. The graph G_b is computed batch-wise and is used to compute the Laplacian matrix L_b and eigenvector matrix U_b . The latent space of the network is k -dimensional therefore k smallest eigenvectors are selected in U_k . Q_N and K_N networks are used to compute S_b .

the spectral embedding $U_k^\top(i)$ in the least squares sense. Due to the convexity enforced by elastic-net regularization, the optimization of the proposed loss is more stable and robust in the presence of noise.

Orthogonality on the rows of the matrix Z_b may also be enforced during network training. Since each row of Z_b corresponds to an eigenvector of L_b , therefore each row of Z_b is normalized to the unit norm and constrained to be orthogonal to other rows:

$$\mathcal{L}_O := \min_{\theta_e, \theta_d} \sum_{i=1}^m (||x_i - \hat{x}_i||_2 + \lambda_1 ||z_i - U_k^\top(i)||_1 + \lambda_2 ||z_i - U_k^\top(i)||_2 + \lambda_3 ||Z_b^\top z_i - I_b(i)||_F^2) \quad (6)$$

The spectral embedding does not ensure the input space structure is preserved in the latent space. To this end, we propose a self-expression matrix-based loss function to be simultaneously minimized with the spectral embedding-based loss. In manifold learning, it has been observed that manifold properties may be invariant to some projection spaces [51]. We aim to find a spectral projection preserving input data structure. For this purpose, a structure-preserving loss simultaneously along with spectral embedding loss is minimized. A pre-computed batch-based self-expressive matrix S_b in the input space is utilized for this purpose. The spectral embedding is forced to preserve the input data structure by minimizing

the following loss:

$$\mathcal{L}_H := \min_{\theta_e, \theta_d} \sum_{i=1}^m (||x_i - \hat{x}_i||_2 + \lambda_1 ||z_i - U_k^\top(i)||_1 + \lambda_2 ||z_i - U_k^\top(i)||_2 + \lambda_3 ||Z_b^\top z_i - I_b(i)||_F^2 + \lambda_4 ||z_i - Z_b S_b(i)||_F^2) \quad (7)$$

where $S_b(i)$ is a column of S_b , which is self-expressive representation of data point x_i in the input space.

C. Attention-Based Self-expressive Matrix Learning

Inspired by the self-attention model in transformer networks, a batch-based self-expressive matrix \mathcal{H}_b is learned using two fully connected learnable networks Q_N and K_N [61, 82]. Given a query data point x_i which needs to be synthesized using remaining key data points x_j in that batch, where $j \neq i$, we forward x_i through Q_N : $\bar{x}_i = Q_N(x_i) \in \mathcal{R}^t$ and all x_j through K_N : $\bar{x}_j = K_N(x_j) \in \mathcal{R}^t$. Attention score between \bar{x}_i and \bar{x}_j is used to get self-expressive coefficients: $\mathcal{H}_b(i, j) = \bar{x}_i^\top \bar{x}_j$. To learn the parameters of Q_N and K_N , the following objective function is minimized:

$$\min_{\theta_Q, \theta_K} \gamma ||x_i - X_i \mathcal{H}_b(i)||_2^2 + \beta ||\mathcal{H}_b(i)||_1 + (1 - \beta) ||\mathcal{H}_b(i)||_2, \quad (8)$$

where $X_i = [x_1, x_2, \dots, x_{i-1}, \mathbf{0}, x_{i+1}, \dots, x_m]$ contains the batch data except x_i , $\mathcal{H}_b(i)$ is the i -th column of \mathcal{H}_b , $\gamma > 0$ and $1 \geq \beta \geq 0$. In Eq. (8) elastic-net regularizer [77] is used to avoid over-segmentation in \mathcal{H}_b . Once \mathcal{H}_b is learned, a sparse binary coefficient matrix S_b is computed using KNN algorithm. For each query x_i only the coefficients corresponding to the few nearest neighbors are retained as 1.00, while

the remaining coefficients are suppressed to 0.00. Thus \mathcal{S}_b is made sparse enabling only a few nearest neighbors of x_i to contribute. Our choice of batch-wise training of Q_N and K_N , for the computation of \mathcal{H}_b , is scalable to larger datasets and also computationally efficient, and memory requirement is reduced compared to full-scale implementations.

IV. EXPERIMENTAL EVALUATIONS

We extensively evaluated the proposed structure-aware deep spectral embedding (SADSE) algorithm on six publicly available datasets including EYaleB [12], Coil-100 [44], MNIST [28], ORL [52], CIFAR-100 [27], and ImageNet-10 [7], and compare with fifty one existing state-of-the-art approaches including EDESC [5], PSSC [41], SENet [82], NCSC [83], DCFSC [54], S³COMP-C [8], ODSC [59], SR-SSC [2], SSCOMP [78], EnSC-ORGEN [77], DSC [20], DEPICT [14], Struct-AE [48], DASC [84], S²Conv-SCN [81], MLRDSC [25], MLRDSC-DA [1], S⁵C [43], SC-LALRG [75], KCRSC [67], SpecNet [55], ACC_CN [32], DLRSC [24], RGRL-L2 [23], MESC-Net[49], RED-SC [74], RCFE [36], FTRR [42], Cluster-GAN [13], SSRSC [72], S²ESC [85], DSC-DL[19], DAE [62], IDEC [15], DCGAN [50], DeCNN [80], VAE [26], ADC [16], AE [3], DEC [71], DAC [7], IIC [21], DCCM [68], PICA [19], CC [33], SPICE [45], JULE [73], DDC [6], SCAN [60], PCL [30], and TCL [35].

For all datasets, we experimented with two settings including full data to be used as train and test, SADSE_F, and using an unseen 20% test data, referred to as SADSE_T. The proposed approach is compared with SOTA using the measures used by the original authors including classification accuracy (Acc.) and normalized mutual information (NMI). A detailed ablation study is also performed to show the effectiveness of each proposed component.

A. Experimental Settings

In all of our experiments, we used a four-layer encoder-decoder network with ‘tanh’ activation function. First of all, the full network is trained for 100 epochs using only the reconstruction loss then the encoder network is trained using the remaining proposed losses with Adadelta [79] optimizer and a learning rate of $1e^{-3}$. For all experiments, the encoder network is further trained for 1000 epochs. The hyperparameters in Eq. (7) are empirically set to $\lambda_1 = \lambda_3 = 0.002$, $\lambda_2 = \lambda_4 = 0.02$ in all experiments. Each of Q_N and K_N is an FC network with three layers beyond the input layer of size {1024,1024,1024} and is trained batch by batch. KNN algorithm is then used with 3-nearest neighbors for all datasets. Adam optimizer with a learning rate of $1e^{-3}$, $\beta = 0.9$, and $\gamma = 200$ are used for the training of Q_N and K_N in all experiments. **As a linear clustering method, K-means is employed.**

B. Evaluations on Different Datasets

EYaleB dataset contains 64 images having size 192×168 of each of the 38 subjects under 9 different illumination conditions [29]. Following the other SOTA methods, we consider only 2432 frontal face images which are then randomly split

Methods	EYALEB		MNIST	
	Acc.	NMI	Acc.	NMI
S ⁵ C [43]	60.70	-	59.60	-
SSCOMP [78]	77.59	83.25	-	-
SC-LALRG [75]	79.66	84.52	78.20	76.01
KCRSC [67]	81.40	88.10	64.70	64.30
S ³ COMP-C [8]	87.41	86.32	96.32	-
FTRR [42]	-	-	70.70	66.72
PSSC _i [41]	-	-	78.50	72.76
PSSC [41]	-	-	84.30	76.76
DCFSC [54]	93.87	-	-	-
Struct-AE [48]	94.70	-	65.70	68.98
DEC [71]	-	-	84.30	-
IDEC [15]	-	-	88.06	86.72
SR-SSC [2]	-	-	91.09	93.06
EDESC [5]	-	-	91.30	86.20
EnSC-ORGEN [77]	-	-	93.79	-
NCSC [83]	-	-	94.09	86.12
DSC-Net-L1 [20]	96.67	-	-	-
ACC_CN [32]	97.31	99.34	78.60	74.21
DSC-Net-L2 [20]	97.33	-	-	-
DLRSC [24]	97.53	-	-	-
RGRL-L2 [23]	97.53	96.61	81.40	75.52
ODSC [59]	97.78	-	81.20	-
MESC-Net[49]	98.03	97.27	81.11	82.26
Cluster-GAN [13]	-	-	96.40	92.10
DEPICT [14]	-	-	96.50	91.70
SENet [82]	-	-	96.80	91.80
SpecNet [55]	-	-	97.10	92.40
S ² Conv-SCN-L2 [81]	98.44	-	-	-
S ² Conv-SCN-L1 [81]	98.48	-	-	-
RED-SC [74]	98.52	-	74.34	73.16
DASC [84]	98.56	98.01	80.40	78.00
MLRDSC [25]	98.64	-	-	-
DSC-DL[19]	98.90	97.40	81.20	76.10
MLRDSC-DA [1]	99.18	-	-	-
SADSE _F	99.95	99.95	97.35	92.81

TABLE I: Comparison of the proposed SADSE_F algorithm with existing SOTA on the EYaleB and MNIST datasets using full data as train and test.

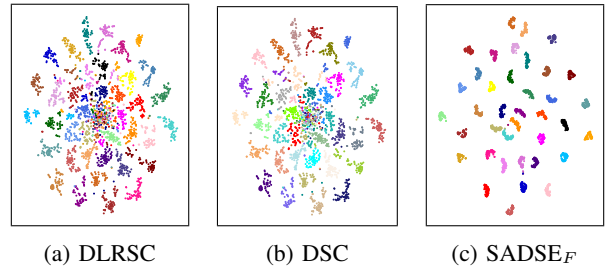


Fig. 2: Visual cluster compactness comparison of the proposed SADSE_F algorithm with SOTA methods using t-SNE on EYaleB dataset

into 1946/486 train/test splits in SADSE_T. Deep features are extracted from the second last layer of Densenet-201 and then PCA is used to reduce dimensions to 784. A batch size of 486 is used. The proposed SADSE_F algorithm has obtained the best accuracy of 99.95%, outperforming the compared methods as shown in Table I. Fig. 2 shows the visual comparison of the proposed SADSE algorithm with compared methods on this dataset. All 2432 images are plotted using the t-SNE algorithm by assigning each cluster a different color. The clusters obtained by the proposed SADSE algorithm are more compact than the compared methods.

Methods	Acc.	NMI
S ⁵ C [43]	54.10	-
DSC-Net-L1 [20]	66.38	-
DSC-Net-L2 [20]	69.04	-
EnSC-ORGEN [77]	69.24	-
DLRSC [24]	71.86	-
MESC-Net [49]	71.88	90.76
S ² Conv-SCN-L2 [81]	72.17	-
DCFSC [54]	72.70	-
S ² Conv-SCN-L1 [81]	73.33	-
MLRDSC [25]	76.72	-
S ³ COMP-C [8]	78.89	-
MLRDSC-DA [1]	79.33	-
RCFE [36]	79.63	96.23
SADSE _F	84.95	93.91

TABLE II: Comparison of the proposed SADSE_F algorithm with existing SOTA methods on Coil-100 dataset.

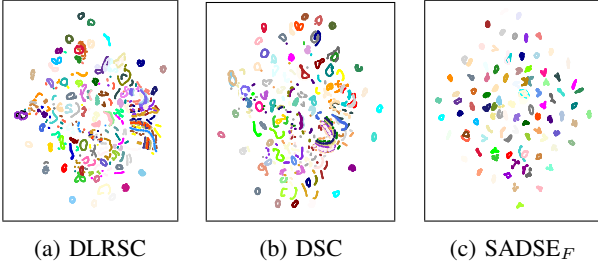


Fig. 3: Visual cluster compactness comparison of the proposed SADSE_F with SOTA methods using t-SNE on Coil-100 dataset.

Coil-100 dataset has 7200 gray-scale images having size 128×128 of 100 different objects taken at pose intervals of 5 degrees. Deep features are extracted from the second last layer of DenseNet-201 and then PCA is used to reduce dimensionality to 3000. We used a batch size of 720, and a random train/test split of 5760/1440 in SADSE_T. The proposed SADSE_F has obtained an accuracy of 84.95% outperforming SOTA methods as shown in Table II. Fig. 3 shows a visual comparison of cluster compactness for different algorithms.

Training stability of SADSE algorithm: In Fig. 4, we compare the training performance stability of different SOTA methods on EYaleB and Coil-100 datasets, respectively. The existing compared methods were trained using a single batch over the full dataset in each epoch while SADSE is trained using 5 batches for EYaleB and 10 batches for Coil-100 in each epoch. Despite batch-based training, the proposed method does not fluctuate much compared to the SOTA methods. The stability of SADSE demonstrates better convergence as the model gets trained.

MNIST dataset consists of 70000 grayscale images of size 28×28 with 10 different classes [28]. For this dataset, we computed scattered convolutional features using [4] as a pre-processing step, as used by other SOTA [8]. PCA is then used to reduce dimensionality to 2000 and a batch size of 500 is used. The standard 60000/10000 train/test split is used in SADSE_T. The proposed SADSE_F has obtained an accuracy of 97.35% compared to SOTA methods as shown in Table I.

ORL dataset contains 400 face images of size 112×92 of 40 different subjects, where each subject presents 10 images of different facial expressions under varying light conditions [52].

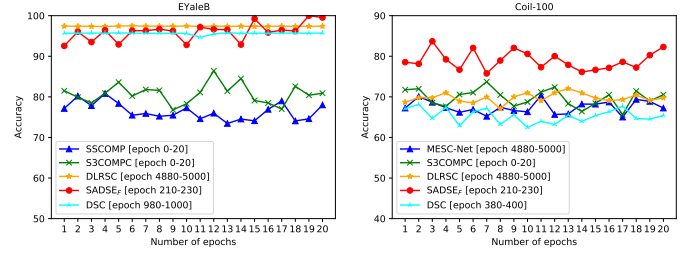


Fig. 4: Stability comparison of SADSE_F with different SOTA methods during training on EYaleB and Coil-100.

Methods	Acc.	NMI
KCRSC [67]	72.30	86.30
SSRSC [72]	78.25	-
DCFSC [54]	85.20	-
PSSC _l [41]	85.25	92.58
DSC-Net-L1 [20]	85.75	-
DSC-Net-L2 [20]	86.00	-
RED-SC [74]	86.13	91.16
PSSC [41]	86.75	93.49
DASC [84]	88.25	93.15
S ² Conv-SCN-L2 [81]	88.75	-
MLRDSC [25]	88.75	-
S ² ESC [85]	89.00	93.52
S ² Conv-SCN-L1 [81]	89.50	-
SADSE _F	90.75	94.66

TABLE III: Comparison of the proposed SADSE_F algorithm with existing SOTA methods on ORL dataset.

The dataset exhibits face images with open or closed eyes, wearing glasses or not, and having a smile or not. A random train/test split of 320/80 is used in SADSE_T. Deep features are extracted from the second last layer of DenseNet-121 and PCA is used to reduce dimensionality to 400 with a batch size of 400. The proposed SADSE_F has obtained an accuracy of 90.75% outperforming SOTA methods as shown in Table III.

CIFAR-100 dataset contains 60000 different object images of size 32×32 of 100 different subjects, categorized into 20 super-classes which are considered as ground-truth [27]. A random train/test split of 50000/10000 is used in SADSE_T. Deep features of dimension 512 are extracted from the second last layer of the baseline algorithm which is Contrastive Clustering (CC) [33] for this dataset. A batch size of 1000 is used in these experiments. The proposed SADSE_F has

Datasets	Methods	Acc.	NMI	F1 score	Precision
EYaleB	SADSE _F	99.95	99.95	99.95	99.95
	SADSE _T	99.95	99.95	99.95	99.95
Coil-100	SADSE _F	84.95	93.91	84.95	84.57
	SADSE _T	86.04	94.17	86.04	86.26
MNIST	SADSE _F	97.35	92.81	97.35	97.35
	SADSE _T	97.43	93.23	97.43	97.43
ORL	SADSE _F	90.75	94.66	90.75	92.61
	SADSE _T	87.50	95.91	87.50	88.75
CIFAR-100	SADSE _F	47.75	45.77	47.75	47.86
	SADSE _T	47.79	46.47	47.79	52.30
ImageNet-10	SADSE _F	91.69	87.53	91.69	91.78
	SADSE _T	90.43	87.33	90.43	90.55

TABLE IV: Performance comparison of the proposed SADSE_T algorithm over unseen test split and full dataset used for both training and testing (SADSE_F).

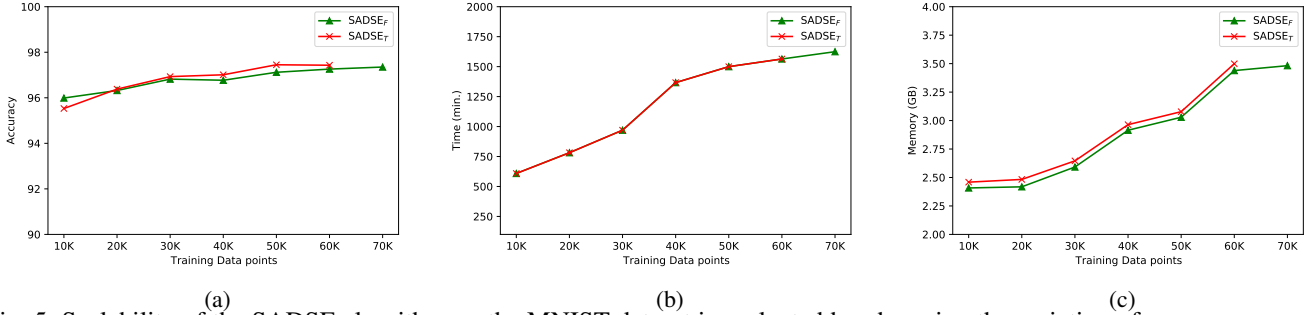


Fig. 5: Scalability of the SADSE algorithm on the MNIST dataset is evaluated by observing the variation of accuracy, execution time, and memory consumption, by increasing dataset size. This experiment shows SADSE algorithm is scalable to larger datasets.

Methods	CIFAR-100		ImageNet-10	
	Acc.	NMI	Acc.	NMI
DAE [62]	15.1	11.1	30.4	20.6
DCGAN [50]	15.1	12.0	34.6	22.5
DeCNN [80]	13.3	9.2	31.3	18.6
JULE [73]	13.7	10.3	30.0	17.5
VAE [26]	15.2	10.8	33.4	19.3
ADC [16]	16.0	-	-	-
AE [3]	16.5	10.00	31.7	21.0
DEC [71]	18.5	13.6	38.1	28.2
DAC [7]	23.8	18.5	52.7	39.4
IIC [21]	25.7	-	-	-
DCCM [68]	32.7	28.5	71.0	60.8
PICA [19]	33.7	31.0	87.0	80.2
CC [33]	42.9	43.1	89.3	85.9
SPICE [45]	46.8	44.8	(96.9)	(92.7)
SCAN [60]	48.3	48.5	-	-
PCL [30]	52.6	52.8	90.7	84.1
TCL [35]	53.1	52.9	89.5	87.5
SADSE _F	47.75	45.77	91.69	87.53

TABLE V: Comparison of the proposed SADSE_F with existing SOTA methods on CIFAR-100 and ImageNet-10 datasets. "()" denotes that pre-training was done using labeled data.

obtained an accuracy of 47.75% which is 4.85% better than the baseline CC. It is also better than SPICE, PICA, IIC, and many other methods as shown in Table V. Some methods such as TCL, PCL, SCAN have obtained even better performance which may be attributed to careful fine-tuning after contrastive clustering.

ImageNet-10 dataset [7] contains 13000 different object images of size 224×224 of 10 objects chosen from ILSVRC2012 1K [10]. A random train/test split of 10000/3000 is used in SADSE_T while SADSE_F is trained/tested on the full dataset. The same deep features and batch size are employed as in the CIFAR-10 dataset. The proposed SADSE_F has obtained an accuracy of 91.69% outperforming SOTA methods as shown in Table V.

C. Generalization to Unseen Data sets

We evaluate our proposed algorithm in train/test splits as SADSE_T, and the full dataset used for both training and testing as SADSE_F. During testing, we don't need to repeat any training step and SADSE_T has achieved better test accuracy on all datasets. Many existing methods such as Struct-AE, DSC, and S³COMP-C have not reported results on unseen

Datasets	DSC		Struct-AE		DLRSC		SADSE _F	
	Time	Mem	Time	Mem	Time	Mem	Time	Mem
EYaleB	201.0	32.1	175.2	10.66	570.4	0.62	107.1	2.18
Coil-100	1653.8	50.6	-	-	3307.6	3.25	458.5	3.58

TABLE VI: Time (min.) and memory (GB) comparison of different SOTA methods with SADSE.

test data. Overall, we used four measures to demonstrate the generalization of the proposed SADSE algorithm to unseen test data points as shown in Table IV. In the ORL dataset, the test/train split is 80/320. Due to the very small training data size, SADSE_T performance is less than SADSE_F. While for the other datasets, its performance is the same or better than the full training dataset.

D. Scalability to Varying Training Data Size

Due to batch-based training, both SADSE_F and SADSE_T are scalable to larger datasets. To demonstrate this, we have used an increase of 10000 data points starting from 10000/60000 train/test splits on MNIST dataset. We observed an increase in the accuracy of SADSE_F as training data points are increased, and when testing the same models for SADSE_T the accuracy on unseen test data splits also increases accordingly (Fig. 5a). We observed an increase in the execution time of the SADSE_F as the training dataset becomes larger, and also for SADSE_T when tested on the unseen same number of data points (Fig. 5b). The memory consumption of SADSE_F increases linearly with an increasing dataset as the model gets trained, and also for SADSE_T when tested on the same number of unseen data points (Fig. 5c). The scalability of our proposed method is exhibited when the accuracy of SADSE_T reaches 95% even when the training data set is only 10000 and all remaining data is used for testing. In Table VI we have also compared execution time (minutes) and memory consumption (GB) of SADSE_F with SOTA methods. Due to batch-based training our proposed method, has consumed fewer memory resources and smaller execution time.

E. Ablation Study

To evaluate the contribution of each loss term in SADSE algorithm, we have performed a detailed ablation study. We

Data sets	Eyaleb	Coil-100	MNIST	ORL
$\mathcal{L}_R + \mathcal{L}_S$	99.95	83.59	95.61	88.75
\mathcal{L}_o	99.95	84.75	96.58	89.00
\mathcal{L}_H	99.95	84.95	97.35	90.75

TABLE VII: Ablation study of the proposed SADSE_F algorithm in terms of classification accuracy. The addition of each loss term has caused an increase in the accuracy of the SADSE_F algorithm.

Datasets	S_b	H_s
EyaleB	99.95	99.95
MNIST	97.35	97.01
Coil-100	84.95	82.26
ORL	90.75	89.25
CIFAR-100	47.75	46.70
ImageNet-10	91.69	92.25

TABLE VIII: Accuracy comparison using S_b and H_s on different datasets.

used different loss terms’ combinations to train our proposed model and report the accuracy of SADSE_F in Table VII. We observe each loss term has contributed an increase in the accuracy, and overall loss term \mathcal{L}_H provides the best accuracy.

Ablation on learning of self-expressive matrix: Many existing methods compute self-expressive matrix \mathcal{H}_s using Lasso for sparse subspace clustering [11, 48]. We implemented the same in a batch fashion to compute \mathcal{H}_s as follows:

$$\min_{\mathcal{H}_s} \|X_b - X_b \mathcal{H}_s\|_F^2 + \lambda \|\mathcal{H}_s\|_1 \quad s.t. \quad \mathcal{H}_s(i, i) = 0, \quad (9)$$

and compared it with self-attention-based S_b . Table VIII shows accuracy results on all datasets when S_b in (7) is replaced by H_s . **Hyper Parameters Tuning:** In order to select the best values of λ_i , $i = \{1, 2, 3, 4\}$ we have performed experiments on MNIST dataset, and accuracy was observed. We observe that for $\lambda_1 = \lambda_2 = \lambda_3 = \lambda_4 = 1$, the accuracy of SADSE_F is 96.23%, and with $\lambda_1 = \lambda_2 = \lambda_3 = \lambda_4 = 0.02$, the accuracy is 96.05%. When we reduce λ_1 and λ_3 ten times smaller than the others ($\lambda_1 = \lambda_3 = 0.002$, $\lambda_2 = \lambda_4 = 0.02$) the accuracy increases to 97.35%. So for all datasets, we used the values of hyperparameters as $\lambda_1 = \lambda_3 = 0.002$, and $\lambda_2 = \lambda_4 = 0.02$. Though, further fine-tuning may increase the accuracy of the proposed algorithm.

Performance variation is observed by varying $k=1-6$ in KNN on EyaleB dataset and the same performance is observed for 3-6 neighbors. Therefore, for all datasets, $k = 3$ is used though fine-tuning may have further improved the results.

V. CONCLUSION

A structure-aware deep spectral embedding (SADSE) algorithm is proposed to learn the spectral representation of input data spanning non-linear manifolds. The proposed SADSE algorithm is based on deep neural networks which are trained by using direct supervision of spectral embedding while preserving the input data structure. The trained network simulates a spectral clustering algorithm including the eigenvector computation of the Laplacian matrix. Therefore the learned representations need not be subjected once again to the traditional spectral clustering as often done by the existing SOTA methods. Thus the learned representations are directly clustered using a linear clustering method such as k-means. To make the learned spectral representation structure

aware, a self-expression matrix is batch-wise computed on the input data. To this end, a self-attention-based global structure encoding technique is proposed using deep neural networks. The learned self-expression matrix is made sparse by using a nearest-neighbor-based approach. The SADSE algorithm is made scalable to larger datasets by applying loss terms in a batch-wise fashion. Our trained network can also estimate spectral representation for unseen data points coming from distributions similar to the training data. Experiments are performed on four publicly available datasets and compared with existing SOTA methods. Our experiments demonstrate the excellent performance of the proposed SADSE algorithm compared to the existing methods.

REFERENCES

- [1] Mahdi Abavisani, Alireza Naghizadeh, Dimitris Metaxas, and Vishal Patel. Deep subspace clustering with data augmentation. *Adv. in Neural Info. Processing Systems*, 33, 2020. 1, 5, 6
- [2] Maryam Abdolali, Nicolas Gillis, and Mohammad Rahmati. Scalable and robust sparse subspace clustering using randomized clustering and multilayer graphs. *Signal Processing*, 163:166–180, 2019. 2, 5
- [3] Yoshua Bengio, Pascal Lamblin, Dan Popovici, and Hugo Larochelle. Greedy layer-wise training of deep networks. *Adv. in Neural Info. Processing Systems*, 19, 2006. 5, 7
- [4] Joan Bruna and Stéphane Mallat. Invariant scattering convolution networks. *IEEE transactions on pattern analysis and machine intelligence*, 35(8):1872–1886, 2013. 6
- [5] Jinyu Cai, Jicong Fan, Wenzhong Guo, Shiping Wang, Yunhe Zhang, and Zhao Zhang. Efficient deep embedded subspace clustering. In *Proceedings of the IEEE/CVF Conference on Computer Vision and Pattern Recognition*, pages 1–10, 2022. 5
- [6] Jianlong Chang, Yiwen Guo, Lingfeng Wang, Gaofeng Meng, Shiming Xiang, and Chunhong Pan. Deep discriminative clustering analysis. *arXiv preprint arXiv:1905.01681*, 2019. 5
- [7] Jianlong Chang, Lingfeng Wang, Gaofeng Meng, Shiming Xiang, and Chunhong Pan. Deep adaptive image clustering. In *Proceedings of the IEEE international conference on computer vision*, pages 5879–5887, 2017. 2, 5, 7
- [8] Ying Chen, Chun-Guang Li, and Chong You. Stochastic sparse subspace clustering. In *Proceedings of the IEEE/CVF Conference on Computer Vision and Pattern Recognition*, pages 4155–4164, 2020. 1, 2, 5, 6
- [9] Madalina Ciortan and Matthieu Defrance. Optimization algorithm for omic data subspace clustering. In *The 12th International Conference on Computational Systems-Biology and Bioinformatics*, pages 69–89, 2021. 1
- [10] Jia Deng, Wei Dong, Richard Socher, Li-Jia Li, Kai Li, and Li Fei-Fei. Imagenet: A large-scale hierarchical image database. In *2009 IEEE conference on computer vision and pattern recognition*, pages 248–255. Ieee, 2009. 7

- [11] E. Elhamifar and R. Vidal. Sparse subspace clustering: Algorithm, theory, and applications. *IEEE Transactions on Pattern Analysis and Machine Intelligence*, 2013. 1, 8
- [12] Athinodoros S. Georghiades, Peter N. Belhumeur, and David J. Kriegman. From few to many: Illumination cone models for face recognition under variable lighting and pose. *IEEE Trans on Pattern Analysis and Mach. Int.*, 23(6):643–660, 2001. 2, 5
- [13] Kamran Ghasedi, Xiaoqian Wang, Cheng Deng, and Heng Huang. Balanced self-paced learning for generative adversarial clustering network. In *Proc. of the Conference on Computer Vision and Pattern Recognition*, pages 4391–4400, 2019. 5
- [14] Kamran Ghasedi Dizaji, Amirhossein Herandi, Cheng Deng, Weidong Cai, and Heng Huang. Deep clustering via joint convolutional autoencoder embedding and relative entropy minimization. In *Proceedings of the IEEE international conference on computer vision*, pages 5736–5745, 2017. 5
- [15] Xifeng Guo, Long Gao, Xinwang Liu, and Jianping Yin. Improved deep embedded clustering with local structure preservation. In *IJCAI*, pages 1753–1759, 2017. 5
- [16] Philip Haeusser, Johannes Plapp, Vladimir Golkov, Elie Aljalbout, and Daniel Cremers. Associative deep clustering: Training a classification network with no labels. In *Pattern Recognition: 40th German Conference, Oct. 9-12.*, pages 18–32, 2019. 5, 7
- [17] Li He, Nilanjan Ray, Yisheng Guan, and Hong Zhang. Fast large-scale spectral clustering via explicit feature mapping. *IEEE transactions on cybernetics*, 49(3):1058–1071, 2018. 2
- [18] R. Hu, L. Fan, and L. Liu. Co, Aesegmentation of 3d shapes via subspace clustering. *Computer graphics forum*, 31(5):1703–1713, 2012. 1
- [19] J Huang, S Gong, and X Zhu. Deep semantic clustering by partition confidence maximisation. In *Pro. Conference on Computer Vision and Pattern Recognition*, 2020. 5, 7
- [20] P. Ji, T. Zhang, H. Li, M. Salzmann, and I. Reid. Deep subspace clustering networks. In *Proc. NIPS*, 2017. 1, 2, 5, 6
- [21] Xu Ji, Joao F Henriques, and Andrea Vedaldi. Invariant information clustering for unsupervised image classification and segmentation. In *Proceedings of the IEEE/CVF International Conference on Computer Vision*, pages 9865–9874, 2019. 5, 7
- [22] Zhao Kang, Zhiping Lin, Xiaofeng Zhu, and Wenbo Xu. Structured graph learning for scalable subspace clustering: From single view to multiview. *IEEE Transactions on Cybernetics*, 2021. 2
- [23] Zhao Kang, Xiao Lu, Jian Liang, Kun Bai, and Zenglin Xu. Relation-guided representation learning. *Neural Networks*, 131:93–102, 2020. 5
- [24] Mohsen Kheirandishfard, Fariba Zohrizadeh, and Farhad Kamangar. Deep low-rank subspace clustering. In *Proceedings of the IEEE/CVF Conference on Computer Vision and Pattern Recognition Workshops*, pages 864–865, 2020. 2, 5, 6
- [25] Mohsen Kheirandishfard, Fariba Zohrizadeh, and Farhad Kamangar. Multi-level representation learning for deep subspace clustering. In *Proceedings of the IEEE/CVF Winter Conference on Applications of Computer Vision*, pages 2039–2048, 2020. 1, 5, 6
- [26] Diederik P Kingma and Max Welling. Auto-encoding variational bayes. *arXiv preprint arXiv:1312.6114*, 2013. 5, 7
- [27] Alex Krizhevsky, Geoffrey Hinton, et al. Learning multiple layers of features from tiny images. 2009. 2, 5, 6
- [28] Yann LeCun, Léon Bottou, Yoshua Bengio, Patrick Haffner, et al. Gradient-based learning applied to document recognition. *Proceedings of the IEEE*, 86(11):2278–2324, 1998. 2, 5, 6
- [29] Kuang-Chih Lee, Jeffrey Ho, and David J Kriegman. Acquiring linear subspaces for face recognition under variable lighting. *IEEE Transactions on Pattern Analysis & Machine Intelligence*, (5):684–698, 2005. 5
- [30] Junnan Li, Pan Zhou, Caiming Xiong, and Steven CH Hoi. Prototypical contrastive learning of unsupervised representations. *arXiv preprint arXiv:2005.04966*, 2020. 5, 7
- [31] Mu Li, Xiao-Chen Lian, James T Kwok, and Bao-Liang Lu. Time and space efficient spectral clustering via column sampling. In *CVPR 2011*, pages 2297–2304. IEEE, 2011. 2
- [32] Xuelong Li, Rui Zhang, Qi Wang, and Hongyuan Zhang. Autoencoder constrained clustering with adaptive neighbors. *IEEE transactions on neural networks and learning systems*, 32(1):443–449, 2020. 5
- [33] Yunfan Li, Peng Hu, Zitao Liu, Dezhong Peng, Joey Tianyi Zhou, and Xi Peng. Contrastive clustering. In *Proceedings of the AAAI Conference on Artificial Intelligence*, volume 35, pages 8547–8555, 2021. 5, 6, 7
- [34] Yeqing Li, Junzhou Huang, and Wei Liu. Scalable sequential spectral clustering. In *Thirtieth AAAI conference on artificial intelligence*, 2016. 2
- [35] Yunfan Li, Mouxing Yang, Dezhong Peng, Taihao Li, Jiantao Huang, and Xi Peng. Twin contrastive learning for online clustering. *International Journal of Computer Vision*, 130(9):2205–2221, 2022. 5, 7
- [36] Zhihui Li, Feiping Nie, Xiaojun Chang, Liqiang Nie, Huaxiang Zhang, and Yi Yang. Rank-constrained spectral clustering with flexible embedding. *IEEE transactions on neural networks and learning systems*, 29(12):6073–6082, 2018. 5, 6
- [37] G. Liu, Z. Lin, S. Yan, J. Sun, Y. Yu, and Y. Ma. Robust recovery of subspace structures by low-rank representation. *IEEE NLM*, 35(1):171–184, 2013. 1
- [38] He J. Liu, W. and S. F. Chang. Large graph construction for scalable semi-supervised learning. In *ICML-10*, pages 679–686, 2010. 3
- [39] C. Y. Lu, H. Min, Z. Q. Zhao, L. Zhu, D. S. Huang, and S. Yan. Robust and efficient subspace segmentation via least squares regression. In *Proc. ECCV*, pages 347–360, 2012. 1
- [40] Feng J. Lin Z. Mei T. Lu, C. and S. Yan. Subspace clustering by block diagonal representation. *IEEE transactions on pattern analysis and machine intelligence*

- (PAMI), 41(2):487–501, 2019. 1
- [41] Juncheng Lv, Zhao Kang, Xiao Lu, and Zenglin Xu. Pseudo-supervised deep subspace clustering. *IEEE Transactions on Image Processing*, 30:5252–5263, 2021. 1, 2, 5, 6
- [42] Zhengrui Ma, Zhao Kang, Guangchun Luo, Ling Tian, and Wenyu Chen. Towards clustering-friendly representations: subspace clustering via graph filtering. In *Proceedings of the 28th ACM International Conference on Multimedia*, pages 3081–3089, 2020. 5
- [43] Shin Matsushima and Maria Brbic. Selective sampling-based scalable sparse subspace clustering. *Advances in Neural Information Processing Systems*, 32:12416–12425, 2019. 5, 6
- [44] SA Nene, SK Nayar, and H Murase. Columbia university image library (coil-20). *Technical Report CUCS-005-96*, 1996. 2, 5
- [45] Chuang Niu, Hongming Shan, and Ge Wang. Spice: Semantic pseudo-labeling for image clustering. *IEEE Transactions on Image Processing*, 31:7264–7278, 2022. 5, 7
- [46] V. M. Patel, H. Van Nguyen, and R. Vidal. Latent space sparse subspace clustering. In *Proc. ICCV*, pages 225–232, 2013. 1
- [47] V. M. Patel and R. Vidal. Kernel sparse subspace clustering. In *Proc. ICIP*, pages 2849–2853, 2014. 1
- [48] X. Peng, J. Feng, S. Xiao, W. Y. Yau, J. T. Zhou, and S. Yang. Structured autoencoders for subspace clustering. *IEEE Transactions on Image Processing*, 27(10):5076–5086, 2018. 2, 5, 8
- [49] Zhihao Peng, Yuheng Jia, Hui Liu, Junhui Hou, and Qingfu Zhang. Maximum entropy subspace clustering network. *IEEE Transactions on Circuits and Systems for Video Technology*, 2021. 5, 6
- [50] Alec Radford, Luke Metz, and Soumith Chintala. Un-supervised representation learning with deep convolutional generative adversarial networks. *arXiv preprint arXiv:1511.06434*, 2015. 5, 7
- [51] Sam T Roweis and Lawrence K Saul. Nonlinear dimensionality reduction by locally linear embedding. *science*, 290(5500):2323–2326, 2000. 4
- [52] Ferdinando S Samaria and Andy C Harter. Parameterisation of a stochastic model for human face identification. In *Proceedings of 1994 IEEE workshop on applications of computer vision*, pages 138–142. IEEE, 1994. 2, 5, 6
- [53] Ali Sekmen and Akram Aldroubi. Subspace and motion segmentation via local subspace estimation. In *2013 IEEE Workshop on Robot Vision (WORV)*, pages 27–33. IEEE, 2013. 1
- [54] Junghoon Seo, Jamyoun Koo, and Taegyun Jeon. Deep closed-form subspace clustering. In *Proceedings of the IEEE International Conference on Computer Vision Workshops*, pages 0–0, 2019. 1, 5, 6
- [55] Uri Shaham, Kelly Stanton, Henry Li, Boaz Nadler, Ronen Basri, and Yuval Kluger. Spectralnet: Spectral clustering using deep neural networks. *ICLR*, 2018. 2, 5
- [56] Jie Shen, Ping Li, and Huan Xu. Online low-rank subspace clustering by basis dictionary pursuit. In *International Conference on Machine Learning*, pages 622–631, 2016. 2
- [57] Qianqian Shi, Bing Hu, Tao Zeng, and Chuanchao Zhang. Multi-view subspace clustering analysis for aggregating multiple heterogeneous omics data. *Frontiers in genetics*, page 744, 2019. 1
- [58] Alain B Tchagang, Fazel Famili, and Youlian Pan. Subspace clustering of dna microarray data: Theory, evaluation, and applications. *International Journal of Computational Models and Algorithms in Medicine (IJCMAM)*, 4(2):1–52, 2014. 1
- [59] Jeya Maria Jose Valanarasu and Vishal M Patel. Over-complete deep subspace clustering networks. In *Proceedings of the IEEE/CVF Winter Conference on Applications of Computer Vision*, pages 746–755, 2021. 1, 2, 5
- [60] Wouter Van Gansbeke, Simon Vandenhende, Stamatios Georgoulis, Marc Proesmans, and Luc Van Gool. Scan: Learning to classify images without labels. In *Computer Vision—ECCV 2020: 16th European Conference, Glasgow, UK, August 23–28, 2020, Proceedings, Part X*, pages 268–285. Springer, 2020. 5, 7
- [61] Ashish Vaswani, Noam Shazeer, Niki Parmar, Jakob Uszkoreit, Llion Jones, Aidan N Gomez, Łukasz Kaiser, and Illia Polosukhin. Attention is all you need. *Advances in neural information processing systems*, 30, 2017. 4
- [62] Pascal Vincent, Hugo Larochelle, Isabelle Lajoie, Yoshua Bengio, Pierre-Antoine Manzagol, and Léon Bottou. Stacked denoising autoencoders: Learning useful representations in a deep network with a local denoising criterion. *Journal of machine learning research*, 11(12), 2010. 5, 7
- [63] Ulrike Von Luxburg. A tutorial on spectral clustering. *Statistics and computing*, 17(4):395–416, 2007. 3
- [64] Tim Wallace, Ali Sekmen, and Xiaofei Wang. Application of subspace clustering in dna sequence analysis. *Journal of Computational Biology*, 22(10):940–952, 2015. 1
- [65] Tong Wang, Junhua Wu, Zhenquan Zhang, Wen Zhou, Guang Chen, and Shasha Liu. Multi-scale graph attention subspace clustering network. *Neurocomputing*, 459:302–314, 2021. 1
- [66] Tongxin Wang, Jie Zhang, and Kun Huang. Generalized gene co-expression analysis via subspace clustering using low-rank representation. *BMC bioinformatics*, 20(7):17–27, 2019. 1
- [67] Xiaobo Wang, Zhen Lei, Hailin Shi, Xiaojie Guo, Xiangyu Zhu, and Stan Z Li. Co-referenced subspace clustering. In *2018 IEEE International Conference on Multimedia and Expo (ICME)*, pages 1–6. IEEE, 2018. 5, 6
- [68] Jianlong Wu, Keyu Long, Fei Wang, Chen Qian, Cheng Li, Zhouchen Lin, and Hongbin Zha. Deep comprehensive correlation mining for image clustering. In *Proceedings of the IEEE/CVF international conference on computer vision*, pages 8150–8159, 2019. 5, 7
- [69] Zizhao Wu, Yunhai Wang, Ruyang Shou, Baoquan Chen, and Xinguo Liu. Unsupervised co-segmentation of 3d shapes via affinity aggregation spectral clustering. *Computers & Graphics*, 37(6):628–637, 2013. 1
- [70] Guiyu Xia, Huaijiang Sun, Lei Feng, Guoqing Zhang,

- and Yazhou Liu. Human motion segmentation via robust kernel sparse subspace clustering. *IEEE Transactions on Image Processing*, 27(1):135–150, 2017. [1](#)
- [71] Junyuan Xie, Ross Girshick, and Ali Farhadi. Unsupervised deep embedding for clustering analysis. In *International conference on machine learning*, pages 478–487, 2016. [5](#), [7](#)
- [72] Jun Xu, Mengyang Yu, Ling Shao, Wangmeng Zuo, Deyu Meng, Lei Zhang, and David Zhang. Scaled simplex representation for subspace clustering. *IEEE Transactions on Cybernetics*, 51(3):1493–1505, 2019. [5](#), [6](#)
- [73] Jianwei Yang, Devi Parikh, and Dhruv Batra. Joint unsupervised learning of deep representations and image clusters. In *Proceedings of the IEEE conference on computer vision and pattern recognition*, pages 5147–5156, 2016. [5](#), [7](#)
- [74] Shuai Yang, Wenqi Zhu, and Yuesheng Zhu. Residual encoder-decoder network for deep subspace clustering. In *2020 IEEE International Conference on Image Processing (ICIP)*, pages 2895–2899. IEEE, 2020. [5](#), [6](#)
- [75] Ming Yin, Shengli Xie, Zongze Wu, Yun Zhang, and Junbin Gao. Subspace clustering via learning an adaptive low-rank graph. *IEEE Transactions on Image Processing*, 27(8):3716–3728, 2018. [1](#), [5](#)
- [76] Chong You, Chi Li, Daniel P Robinson, and René Vidal. Scalable exemplar-based subspace clustering on class-imbalanced data. In *Proceedings of the European Conference on Computer Vision (ECCV)*, pages 67–83, 2018. [2](#)
- [77] Chong You, Chun-Guang Li, Daniel P Robinson, and René Vidal. Oracle based active set algorithm for scalable elastic net subspace clustering. In *Proceedings of the IEEE conference on computer vision and pattern recognition*, pages 3928–3937, 2016. [2](#), [4](#), [5](#), [6](#)
- [78] Chong You, Daniel Robinson, and René Vidal. Scalable sparse subspace clustering by orthogonal matching pursuit. In *Proceedings of the IEEE conference on computer vision and pattern recognition*, pages 3918–3927, 2016. [5](#)
- [79] Matthew D. Zeiler. Adadelta: An adaptive learning rate method. *ArXiv*, abs/1212.5701, 2012. [5](#)
- [80] Matthew D Zeiler, Dilip Krishnan, Graham W Taylor, and Rob Fergus. Deconvolutional networks. In *2010 IEEE Computer Society Conference on computer vision and pattern recognition*, pages 2528–2535. IEEE, 2010. [5](#), [7](#)
- [81] Junjian Zhang, Chun-Guang Li, Chong You, Xianbiao Qi, Honggang Zhang, Jun Guo, and Zhouchen Lin. Self-supervised convolutional subspace clustering network. In *Proceedings of the IEEE Conference on Computer Vision and Pattern Recognition*, pages 5473–5482, 2019. [1](#), [2](#), [5](#), [6](#)
- [82] Shangzhi Zhang, Chong You, René Vidal, and Chun-Guang Li. Learning a self-expressive network for subspace clustering. In *Proceedings of the IEEE/CVF Conference on Computer Vision and Pattern Recognition*, pages 12393–12403, 2021. [1](#), [4](#), [5](#)
- [83] Tong Zhang, Pan Ji, Mehrtash Harandi, Wenbing Huang, and Hongdong Li. Neural collaborative subspace clustering. In *International Conference on Machine Learning*, pages 7384–7393. PMLR, 2019. [1](#), [2](#), [5](#)
- [84] Pan Zhou, Yunqing Hou, and Jiashi Feng. Deep adversarial subspace clustering. In *Proceedings of the IEEE Conference on Computer Vision and Pattern Recognition*, pages 1596–1604, 2018. [1](#), [5](#), [6](#)
- [85] Wenjie Zhu, Bo Peng, and Chunchun Chen. Self-supervised embedding for subspace clustering. In *Proceedings of the 30th ACM International Conference on Information & Knowledge Management*, pages 3687–3691, 2021. [5](#), [6](#)



Hira Yaseen is a Ph.D. fellow in the Center for Robot Vision, Department of Computer Science, Information Technology University, Lahore, Pakistan. Previously she did her BS in Computer Engineering from the University of Engineering and Technology Lahore and her Master's in Computer Science from Comsats University Islamabad. Her research areas include Computer Vision and Machine Learning. During her Ph.D., she is working on unsupervised representation learning, data clustering, and object classification.



Arif Mahmood is a Professor in the Computer Science Department, and Dean Faculty of Sciences at the Information Technology University and also Director of the Center for Robot Vision. His current research directions in Computer Vision are person pose detection and segmentation, crowd counting and flow detection, background-foreground modeling in complex scenes, object detection, human-object interaction detection, and abnormal events detection. He is also actively working in diverse Machine Learning applications including cancer grading and prognostication using histology images, predictive auto-scaling of services hosted on the cloud and the fog infrastructures, and environmental monitoring using remote sensing. He has also worked as a Research Assistant Professor with the School of Mathematics and Statistics, University of Western Australia (UWA) where he worked on Complex Network Analysis. Before that, he was a Research Assistant Professor at the School of Computer Science and Software Engineering, UWA, and performed research on face recognition, object classification, and action recognition.